Subcortical Brain Alterations in Carriers of Genomic Copy Number Variants

Kuldeep Kumar, Ph.D., Claudia Modenato, Ph.D., Clara Moreau, Ph.D., Christopher R.K. Ching, Ph.D., Annabelle Harvey, M.Sc., Sandra Martin-Brevet, Ph.D., Guillaume Huguet, Ph.D., Martineau Jean-Louis, M.Sc., Elise Douard, M.Sc., Charles-Olivier Martin, Ph.D., Nadine Younis, M.Sc., Petra Tamer, M.Sc., Anne M. Maillard, Ph.D., Borja Rodriguez-Herreros, Ph.D., Aurélie Pain, M.Sc., 16p11.2 European Consortium, Simons Searchlight Consortium, Leila Kushan, M.Sc., Dmitry Isaev, M.Sc., Kathryn Alpert, M.Sc., Anjani Ragothaman, M.Sc., Jessica A. Turner, Ph.D., Lei Wang, Ph.D., Tiffany C. Ho, Ph.D., Lianne Schmaal, Ph.D., Ana I. Silva, Ph.D., Marianne B.M. van den Bree, Ph.D., David E.J. Linden, M.D., Michael J. Owen, M.D., Ph.D., Jeremy Hall, Ph.D., F.R.C.Psych., Sarah Lippé, Ph.D., Guillaume Dumas, Ph.D., Bogdan Draganski, M.D., Boris A. Gutman, Ph.D., Ida E. Sønderby, Ph.D., Ole A. Andreassen, M.D., Ph.D., Laura M. Schultz, Ph.D., Laura Almasy, Ph.D., David C. Glahn, Ph.D., Carrie E. Bearden, Ph.D., Paul M. Thompson, Ph.D., Sébastien Jacquemont, M.D.

Objective: Copy number variants (CNVs) are well-known genetic pleiotropic risk factors for multiple neurodevelopmental and psychiatric disorders (NPDs), including autism (ASD) and schizophrenia. Little is known about how different CNVs conferring risk for the same condition may affect subcortical brain structures and how these alterations relate to the level of disease risk conferred by CNVs. To fill this gap, the authors investigated gross volume, vertex-level thickness, and surface maps of subcortical structures in 11 CNVs and six NPDs.

Methods: Subcortical structures were characterized using harmonized ENIGMA protocols in 675 CNV carriers (CNVs at 1q21.1, TAR, 13q12.12, 15q11.2, 16p11.2, 16p13.11, and 22q11.2; age range, 6–80 years; 340 males) and 782 control subjects (age range, 6–80 years; 387 males) as well as ENIGMA summary statistics for ASD, schizophrenia, attention deficit hyperactivity disorder, obsessive-compulsive disorder, bipolar disorder, and major depression.

Results: All CNVs showed alterations in at least one subcortical measure. Each structure was affected by at least two CNVs, and the hippocampus and amygdala were affected by five. Shape analyses detected subregional alterations that were averaged out in volume analyses. A common latent dimension was identified, characterized by opposing effects on the hippocampus/amygdala and putamen/pallidum, across CNVs and across NPDs. Effect sizes of CNVs on subcortical volume, thickness, and local surface area were correlated with their previously reported effect sizes on cognition and risk for ASD and schizophrenia.

Conclusions: The findings demonstrate that subcortical alterations associated with CNVs show varying levels of similarities with those associated with neuropsychiatric conditions, as well distinct effects, with some CNVs clustering with adult-onset conditions and others with ASD. These findings provide insight into the long-standing questions of why CNVs at different genomic loci increase the risk for the same NPD and why a single CNV increases the risk for a diverse set of NPDs.

Am J Psychiatry 2023; 180:685–698; doi: 10.1176/appi.ajp.20220304

Subcortical brain structures play a critical role in cognitive, affective, and social functions (1, 2). Large-scale international neuroimaging studies have shown that major neurodevelopmental and psychiatric disorders (NPDs) (3), including schizophrenia (4), major depressive disorder (MDD) (5), bipolar disorder (6), obsessive-compulsive disorder (OCD) (7), autism spectrum disorder (ASD) (8), and attention deficit hyperactivity disorder (ADHD) (9), are associated with alterations in subcortical structures (10–12). These case-control association studies have revealed small to moderate effect sizes on brain morphometry, which have been interpreted as a consequence of heterogeneity at the level of genetics and brain mechanisms (13–16).

"Genetics-first" studies, in which participants are ascertained based on genetic etiology, can potentially overcome challenges posed by the genetic and mechanistic heterogeneity of behaviorally defined (idiopathic) NPDs (17–19). A growing body of literature demonstrates subcortical

See related features: **Editorial** *by Dr. Wagstyl and Dr. Raznahan (p. 634), and* **CME course** *(online and p. 698)*

volumetric alterations associated with genetic risk for NPDs as conferred by copy number variants (CNVs). CNVs are major contributors to NPDs such as ASD and schizophrenia (15, 20) but show weaker associations with bipolar disorder (21, 22) and MDD (23). Among the CNVs included in this study, the largest increases in risk for schizophrenia have been documented for the 22q11.2 deletion (30- to 40-fold) followed by 16p11.2 duplication (10-fold), 1q21.1 deletion, and 15q11.2 deletion (1.5- to 2-fold) (3, 14, 15). ASD risk is highest for 16p11.2 deletions and duplications (10-fold), followed by 1q21.1 duplications and 22q11.2 duplications (3- to 4-fold) (3, 14, 17, 20). All CNVs affect cognitive ability, to varying degrees (decreases between 2.4 and 28.8 IQ points) (Table 1), with the exception of 15q11.2 and 13q12.12 duplications.

Previous studies have shown that CNVs including 1q21.1-distal (24), 16p11.2-proximal BP4-5 (25), 16p11.2-distal BP2-3 (26), 15q11.2 BP1-BP2 (27), and 22q11.2 (13) affect subcortical structures, with mild to large effect sizes (14). Recent studies have found a significant overlap between subcortical and cortical alterations associated with 22q11.2 deletion carriers and those associated with idiopathic schizophrenia as well as other psychiatric illnesses (13, 28).

Beyond volumetric measurements, shape analyses of subcortical structures can capture differences that are predictive of disease status at a higher granularity (2, 29). Studies have typically focused on thickness, defined by the distance from the medial axis of each structure, and local surface area, which is a measure of surface contraction or expansion (13, 30). Both shape measures have been shown to be highly heritable (31, 32) and have been used to map subcortical variation in schizophrenia (30), ASD (29), MDD (33), and bipolar disorder (34). Thickness is a proxy for subregional volume changes, while the relationship between surface and volume depends on the local curvature of the region (30). For CNVs, subcortical analyses at the vertex level have been performed only in 22q11.2 deletion carriers (13), demonstrating multiple clusters of regional subcortical alterations, which were modulated by psychotic illness.

Overall, little is known about how genetic variants conferring risk for psychiatric conditions affect subcortical structures. Previous neuroimaging studies have mainly focused on individual CNVs, making it challenging to directly compare MRI alterations across CNVs as well as to relate these MRI alterations to the level of disease risk conferred by CNVs. In particular, while multiple CNVs confer risk for the same psychiatric conditions (35, 36), it is unknown whether they are also associated with similar patterns of brain alterations underlain by a common latent dimension. Similarly, it has been shown that a common latent dimension can be identified across psychiatric diagnoses (37), and it is unknown whether a similar dimension may be observed for genetic risk.

Our overall aim in this study was to systematically compare effect sizes and patterns of subcortical alterations associated with rare genetic risk for NPDs. Specifically, we aimed 1) to characterize subcortical volumetric and shape alterations in 11 CNVs, 2) to relate effect sizes of CNVs on subcortical metrics with previously reported effects of CNVs on risk for NPDs, and 3) to identify latent subcortical brain morphometry dimensions across CNVs and NPDs.

To this end, we assembled the largest T_1-weighted brain MRI data set across all recurrent CNVs (N=11) previously associated with varying levels of risk for psychiatric illness (Table 1), and characterized volume, three-dimensional surface, and thickness maps of subcortical structures. Effect sizes for six NPDs (ADHD, ASD, bipolar disorder, MDD, OCD, and schizophrenia) were obtained from previously published studies from the ENIGMA consortium.

METHODS

Participants

Recurrent deletions and duplications were included in the study if 1) the level of association between the CNV and psychiatric conditions (or lack thereof) as well as the effect size on cognitive ability was previously established (15, 17, 20, 21, 38–42) and 2) MRI data were available for at least 20 carriers of the same CNV. This minimum sample size of 20 was established based on the power to detect large effect sizes (14).

Clinically Ascertained Groups

CNV carriers were recruited either after being referred for genetic testing related to the diagnosis of a neurodevelopmental disorder or as the relative (e.g., parent) of a CNV carrier. Control subjects were defined as individuals who did not carry any NPD-associated CNVs.

Unselected Population Group

CNV carriers were identified in the UK Biobank. Control subjects were defined as individuals who did not carry any of the 11 CNVs selected from this study.

Demographic details of the study participants, along with coordinates of each of the 11 CNVs, are provided in Table 1 and in Table S1 in the online supplement. Signed consent was obtained by investigators from each cohort for all participants or their legal representatives prior to the investigation. This study, using an aggregate data set, obtained ethics approval from CHU Sainte-Justine Hospital.

MRI Acquisition and Preprocessing

The data sample included three-dimensional T_1-weighted volumetric brain images at 0.8–1.0 mm isotropic resolution across all sites. MRI parameters for each cohort are detailed in the online supplement.

Subcortical Volume and Shape Segmentation

FreeSurfer, version 5.3.0, was used to segment all scans into seven bilateral subcortical regions of interest: nucleus accumbens, amygdala, caudate, hippocampus, putamen, pallidum, and thalamus. The ENIGMA subcortical shape analysis pipeline (30) (http://enigma.ini.usc.edu/protocols/imaging-protocols/) was then applied to derive two measures of shape morphometry for each subcortical region: 1) the

TABLE 1. Genetic, cohort, and demographic characteristics of participants in the study[a]

Locus	Start-Stop Coordinates (hg19) (Mb)	Type	nGenes	Gene	Ascertainment (Cohorts)	N	Age (years)			Sex (M/F)	Diagnoses (ASD/SZ/ Other)	IQ Point Loss	Odds Ratio (ASD/SZ)
							Mean	SD	Range				
1q21.1	chr1, 146.53–147.39	Del	7	CHDIL	Clinical (BC, CDF, EU, SVIP)	28	29	18	8–73	17/11	1/0/7	15	3.2/6.4
					Nonclinical (UKB)	12	59	7	47–68	5/7	0/1/3		
		Dup			Clinical (BC, CDF, EU, SVIP)	17	35	17	8–65	9/8	1/0/4	25	5.3/2.9
					Nonclinical (UKB)	13	62	6	51–72	9/4			
TAR	chr1, 145.39–145.81	Dup	15	RBM8	Nonclinical (UKB)	31	60	8	48–74	14/17		2.4	
13q12.12	chr13, 23.56–24.88	Dup	5	SPATA13	Nonclinical (UKB)	21	62	8	50–76	11/10		0.6	
15q11.2	chr15, 22.81–23.09	Del	4	CYF1P1	Nonclinical (UKB)	108	65	7	49–78	59/49	0/0/2	5.7	1.3/1.9
		Dup			Nonclinical (UKB)	144	64	7	46–79	77/67	0/0/6	0.9	1.8/1
16p11.2	chr16, 29.65–30.20	Del	27	KCTD13	Clinical (BC, CDF, EU, SVIP)	78	17	11	6–54	36/42		26	14.3/1.1
					Nonclinical (UKB)	4	66	3	63–70	1/3			
		Dup			Clinical (BC, CDF, EU, SVIP)	68	31	15	8–63	29/39	10/1/19	11	10.5/11.7
					Nonclinical (UKB)	7	65	6	53–69	3/4			
16p13.11	chr16, 15.51–16.29	Dup	6	NDE1	Nonclinical (UKB)	50	66	6	51–78	26/24		8.7	1.5/2
22q11.2	chr22, 19.04–21.47	Del	49	AIFM3	Clinical (BC, CDF, UCLA)	68	14	6	6–35	33/35	8/2/31	28.8	32.3/23
		Dup			Clinical (BC, CDF, UCLA)	19	17	13	6–45	6/13	2/0/8	8.3	2/0.2
					Nonclinical (UKB)	7	60	11	48–80	5/2	0/0/1		
Control subjects					Clinical (BC, CDF, EU, SVIP, UCLA)	317	26	14	6–63	142/175	1/0/23		
					Nonclinical (UKB)	465	64	7	47–80	245/220			

[a] CNV chromosomal coordinates are provided in megabases (Mb) with the number of genes encompassed in each CNV and a well-known gene for each locus, to help recognize the CNV. Clinically ascertained participants come from five cohorts, and non–clinically ascertained participants are from the UK Biobank. Age and sex are reported for clinical and nonclinical participants separately. The "diagnoses" column reports the number of participants with ASD, schizophrenia, and "other diagnoses," which include the following: language disorder, major depressive disorder, posttraumatic stress disorder, unspecified disruptive and impulse control and conduct disorder, social anxiety disorder, social phobia disorder, speech sound disorder, moderate intellectual disability, specific learning disorder, gambling disorder, bipolar disorder, conduct disorder, attention deficit hyperactivity disorder, substance use disorder, global developmental delay, motor disorder, obsessive-compulsive disorder, sleep disorder, Tourette's disorder, mood disorder, eating disorder, transient tic disorder, trichotillomania, pervasive developmental disorder not otherwise specified, specific phobia, body dysmorphic disorder, mathematics disorder, and dysthymic disorder. IQ point loss and odds ratio for autism spectrum disorder and schizophrenia risk were extracted from previous reports (3, 51). Detailed demographic characteristics are reported in Table S1 in the online supplement. ASD=autism spectrum disorder; BC=Brain Canada (University of Montreal); CDF=Cardiff University; Del=deletion; Dup=duplication; EU=16p11.2 European Consortium; nGenes=number of genes encompassed by the CNV; SVIP=Simons Variation in Individuals Project; SZ=schizophrenia; UCLA=University of California, Los Angeles; UKB=UK Biobank.

radial distance, which is the distance from each vertex to the medial curve of each region (referred to as thickness), and 2) the logarithm of the Jacobian determinant (LogJacs), which corresponds to the surface dilation ratio between the subject structure and the template (referred to as surface). See the online supplement for details.

Quality Control

Visual quality inspection was performed by the same rater using the ENIGMA standardized quality control protocol (13). See the online supplement for details.

Normative Modeling

Changes in brain measures with age (in control subjects; age range, 6–80 years) were modeled using Gaussian processes (43) and were compared with linear models (Figure 1; see also Figure S5B in the online supplement). In subsequent analyses, we used Gaussian process regression (GPR, fitting a model on control subjects and using age, sex, site, and intracranial volume [ICV] as covariates) to obtain W scores (GPR-based Z scores with respect to the mean and standard deviation modeled in control subjects; see Figure S1 in the online supplement). See the online supplement for details.

Statistical Analysis

Linear regression models (using R, version 3.6.3) were used to compute CNV-control differences (Cohen's d) for each CNV using GPR-based W scores. This approach was used for CNVs across ICV, subcortical volumes, and subcortical shape analysis. The false discovery rate (FDR) procedure (44) was applied within CNVs (11 CNVs by eight MRI volumes). For subcortical shape analysis, the FDR procedure was applied

FIGURE 1. Normative age modeling and subcortical volume effect sizes[a]

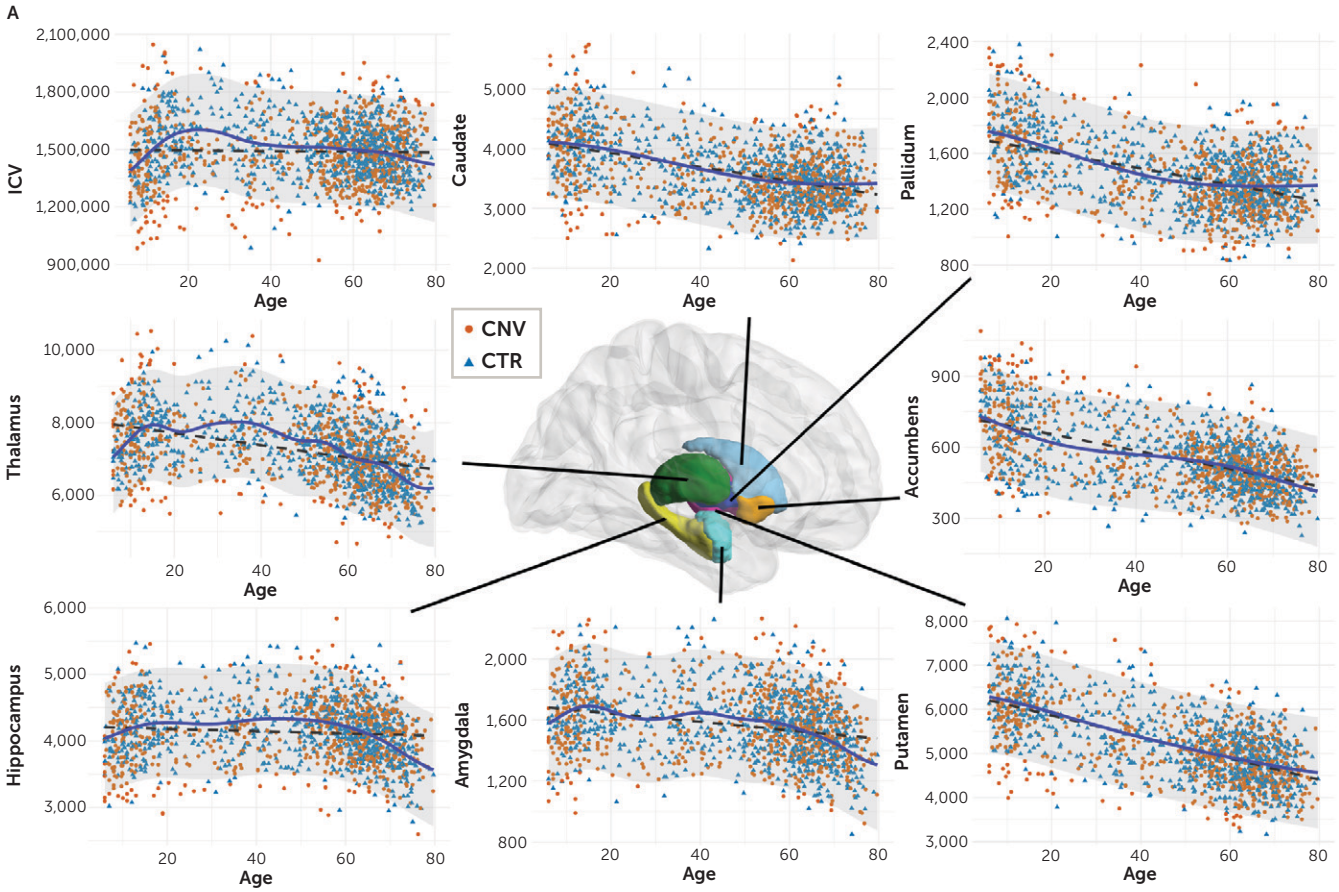

[a] In panel A, scatterplots show the distribution of intracranial volume (ICV) and subcortical volumes with age, along with Gaussian process modeling (solid line) and a linear model (dotted line). Control subjects (used for Gaussian process modeling) and copy number variant carriers are shown as points. Panel B lists Cohen's d values for 11 CNVs for subcortical structures and ICV. Case-control differences were calculated (*lm* function in R) using W scores (derived from Gaussian process modeling); the W score already includes adjustments for age, sex, site, and ICV. Significant effect sizes with nominal p values <0.05 are in boldface, and FDR-corrected p values <0.05 are shown with an asterisk; FDR correction was applied across all CNVs and structures. Darker colors represent higher positive or negative effect sizes. Sample sizes for each analysis (for ICV) are reported in parentheses in the x-axis labels. Detailed effect sizes, standard error, and p values are reported in Figure S2 in the online supplement. CNV=CNV carriers; CTR=control subjects; DEL=deletions; DUP=duplications; FDR=false discovery rate; ICV=intracranial volume.

across 11 CNVs by 27,000 vertices. The significance threshold was set at an FDR-corrected q of 0.05. See the online supplement for additional details.

Effect Sizes

Cohen's d values were computed based on case-control linear regression. Cohen's d values for NPDs were extracted from previous ENIGMA studies (4–9), referred to here as ENIGMA's Cohen's d (see the online supplement). All effect sizes were computed after regressing for age, sex, site, and ICV.

For comparisons across metrics, the following maximum effect sizes were used: absolute Cohen's d for ICV, maximum absolute Cohen's d across seven subcortical volumes, and average absolute Cohen's d of the top decile across subcortical shape vertices. Because the proportion of significant vertices varied across CNVs and NPDs (due to differences in effect and sample sizes) we chose to focus on the top decile of Cohen's d values for all CNVs and NPDs to avoid biases and to provide effect sizes comparable across CNVs and NPDs. Vertices in the top decile were identified for thickness and surface separately and were not constrained by spatial continuity. Statistical testing of spatially correlated Cohen's d profiles was performed using BrainSMASH (45, 46). See the online supplement for details.

Quantifying Shared Variance Across CNVs and NPDs

Principal component analysis quantified shared variance across all CNVs and NPDs. For volume, we used CNV and NPD maps (z-scored Cohen's d contrasts adjusted for ICV and nuisance variables); for vertices, we stacked the thickness and surface maps and ran a single analysis (using the *FactoMineR* package in R). As a sensitivity analysis, we ran separate analyses for CNVs and for NPDs (see Figure S11 in the online supplement). For additional details and methods, see the online supplement.

RESULTS

Effects of CNVs on Subcortical Volumes

Six of the 11 CNVs had significant effects on ICV. Opposing effects were observed for deletions and duplications at the same loci for 1q21.1-distal, 15q11.2, 16p11.2-proximal, and 22q11.2 (Figure 1B). Nine of the 11 CNVs had significant effects on subcortical volumes. The largest effects were observed for 22q11.2 deletions, followed by 16p11.2-proximal, 1q21.1-distal deletions and 1q21.1-distal, 16p11.2-proximal duplications (Figure 1B). Every structure was affected by at least two CNVs, and the hippocampus and amygdala were affected by five CNVs.

Sensitivity analysis testing the effect of 1) the presence or absence of a psychiatric diagnosis, 2) site effects, and 3) averaging left and right subcortical volumes demonstrated that the results were robust (see Figures S3–S5 in the online supplement). In addition, the Cohen's d values for 22q11.2 deletions showed high concordance ($r=0.93$, $p=0.002$) with previously published results from a much larger overlapping sample (13) (N=68 vs. N=430 deletion carriers; see Figure S5A in the online supplement).

Effects of CNVs on Thickness and Local Surface Area

To provide a more refined analysis of subcortical structures, we used thickness (radial distance) and surface (local surface area dilation/contraction). Shape analysis detected significant group differences across all CNVs, with both higher and lower thickness and local surface area relative to the control groups (Figure 2; see also Figure S6 in the online supplement). The CNV-control analyses for 22q11.2 deletions and TAR duplications provided the highest and lowest number of significant vertices, respectively (see Tables S4–S7 in the online supplement). For each CNV, the largest number of significant vertices was observed for thickness in the caudate and for surface in the thalamus, hippocampus, and caudate (see Tables S4–S7 in the online supplement). A significant mirror effect at the vertex level was observed between deletions and duplication for only one locus (16p11.2).

Because surface and thickness showed a positive correlation across most vertices in control subjects, we present a simplified map representing concordant effects on surface and thickness (see Figure S7 in the online supplement). Vertices with the largest concordant increases were observed in the thalamus for 16p11.2-proximal deletions and in the head of the caudate for the 22q11.2 deletions. The largest concordant decreases were observed in the body and tail of the caudate, the tail of the thalamus for 16p11.2-proximal duplications, and both the head and tail of the hippocampus for 22q11.2 deletions (see Table S8 in the online supplement).

Effect sizes of CNVs on thickness and surface were concordant with those reported for volume (concordance correlation coefficients, 0.68 [$p=0.006$] and 0.57 [$p=0.02$], respectively), but were higher on average (bias factor, 0.88 and 0.85, respectively) (see Figure S9 and Table S3 in the online supplement).

CNV Effect Sizes on Subcortical Volume/Shape, Cognition, and Risk for Disease

We found that the effect sizes of CNVs on subcortical volume, thickness, and surface were two- to sixfold larger than those previously published in the ENIGMA studies of idiopathic ADHD, ASD, bipolar disorder, MDD, OCD, and schizophrenia in volume and of MDD and schizophrenia in shape metrics (e.g., the largest effects for 22q11.2 deletion/schizophrenia were 0.92/0.46 for volume, 1.03/0.39 for thickness, and 1.24/0.34 for surface; see Table S2 in the online supplement).

We then investigated whether CNV effect sizes were related to their effects on cognition and disease risk. We observed a significant correlation between the effect size of CNVs on subcortical volume, thickness, and surface and their previously reported effect size on IQ (3, 38, 47) (r values, 0.66–0.75; p values, <0.03) as well as risk for either ASD (3, 20, 48, 49) or schizophrenia (3, 15, 49) (r values, 0.69–0.89; p values, <0.03) (Figure 2C). The results were comparable after

FIGURE 2. Cohen's d maps for subcortical shape analysis and effect size comparison[a]

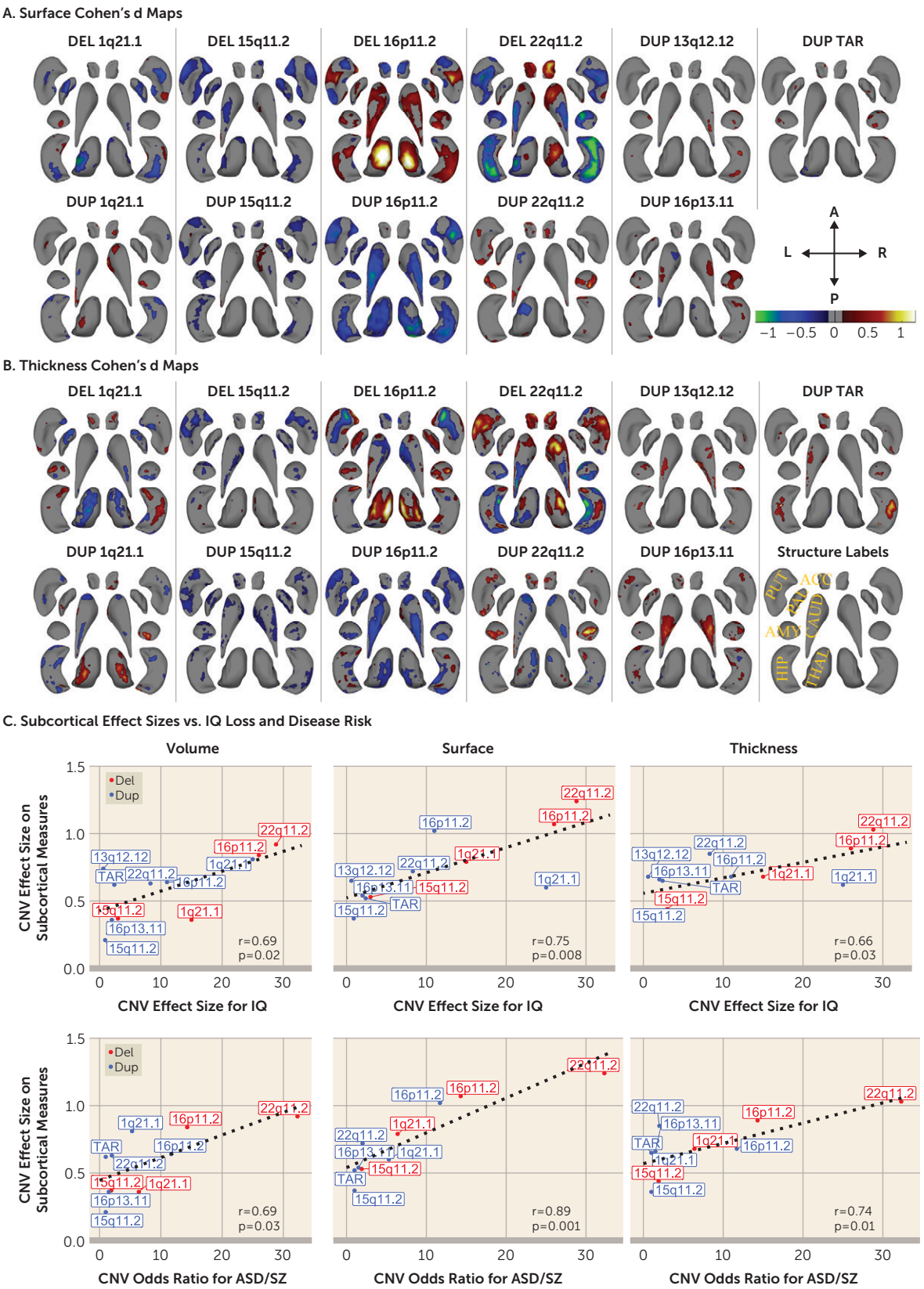

[a] Panels A and B are Cohen's d maps of subcortical shape alterations in surface and thickness, respectively, for 11 CNVs (dorsal view). Significant vertices are shown after applying FDR correction (<0.05) across all 27,000 vertices × 11 CNVs (within each panel). The color bar and dorsal view directions for panels A and B are shown in panel A, and the structures' labels are shown in panel B. Thickness represents local radial distance, and surface represents local

the exclusion of 22q11.2 loci (see Figure S8 in the online supplement). Effect size on subcortical structure was also correlated with the gene content (measured by probability of being loss-of-function intolerant [pLI] or number of genes) of each CNV (see Figure S9 in the online supplement). On the other hand, CNV effect sizes on ICV were not significantly associated with cognition (see Figure S9 in the online supplement).

Comparing Cohen's d Profiles of CNVs and NPDs

Because CNVs are pleiotropic, conferring risk for multiple neuropsychiatric conditions (50), we investigated whether there were any similarities between profiles of subcortical alterations across CNVs and NPDs. We correlated subcortical volume effect sizes across CNVs and NPDs and performed a hierarchical clustering analysis (using Ward's method). Schizophrenia was part of a cluster that included bipolar disorder, MDD, OCD, 22q11.2 deletions, and 1q21.1-distal duplications. This cluster was negatively correlated with the cluster encompassing ASD, 16p11.2-proximal deletions, 15q11.2 deletions, 15q11.2 duplications, and 13q12.12 duplications. ADHD did not cluster with any of the conditions or CNVs (Figure 3A).

However, there was no clear relationship between the level of ASD or schizophrenia risk conferred by CNVs and their clustering with those two conditions (correlation between CNV risk for ASD and CNV-ASD clustering: $r=-0.14$, $p=0.7$; correlation between CNV risk for schizophrenia and CNV-schizophrenia clustering: $r=0.59$, $p=0.07$) (see Figure S11 in the online supplement).

Subcortical Latent Dimensions Across CNVs and NPDs

To investigate the clusters observed above, we performed a principal component analysis on profiles of subcortical volume effect sizes. The first two principal components (PCs) explained 45% and 28% of the variance in Cohen's d values, which was higher than what is expected by chance (see Figure S16 in the online supplement). Dimension 1 of the NPDs and CNVs showed positive and negative loadings for the basal ganglia (pallidum, putamen) and limbic system (thalamus, hippocampus, amygdala), respectively (Figure 3C). The second PC dimension was characterized by the accumbens and thalamus loading on both extremes. Five clusters were obtained by running K-means clustering using PC1 and PC2, with cluster 3 corresponding to adult NPDs, clusters 4 and 5 corresponding to ADHD and ASD, respectively, and clusters 1 and 2 to CNVs. These groupings were reflected in the correlation matrix of Cohen's d profiles (Figure 3A). To test whether CNVs and NPDs separately resulted in similar dimensions, we performed independent principal component analyses on NPDs and CNVs. Latent dimensions (PCs) of both analyses were highly correlated with each other (r values, -0.93 to -0.83) (see Figure S12 in the online supplement).

Latent Dimensions Across Subcortical Shape Metrics of CNVs and NPDs

To understand potentially shared and distinct effects across CNVs, we performed a multivariate analysis (principal component analysis) on Cohen's d maps of both subcortical thickness and local surface area for 11 CNVs, and ENIGMA maps for schizophrenia and MDD (Figure 4; see also Figure S13 in the online supplement). Given data availability, only schizophrenia and MDD were included here. The two first PCs explained 35% of the variance, which was higher than what is expected by chance (see Figure S16 in the online supplement).

PCs identified positive and negative loadings for regions within the same structures. Ventral and dorsal regions showed distinct patterns of alterations. Alterations were mostly bilateral except for the thalamus. As an example, for PC1, vertices with concordant effects (same directionality for thickness and surface) suggested a decrease in subregional volumes of the body and an increase in the head and tail of the caudate. For the hippocampus, most vertices with concordant alterations suggested a volume decrease in the body, but focal increases were also observed in the head (PC1) and tail (PC2) (Figure 4E–H; see also Table S9 in the online supplement).

Comparing principal component analysis results across subcortical metrics shows that structures contributing to the latent dimension for volume are, on average, also those contributing to latent dimension for surface and thickness (see Figure S14 in the online supplement). Lower variance explained for shape analyses suggests that shared Cohen's d profiles may decrease when moving from gross volume to measures with higher granularity (see Figures S15

surface area dilation or contraction. Blue and green indicate negative coefficients, or regions with reduced thickness in the CNV group compared with the control group. Red and yellow indicate positive coefficients, or regions with increased thickness in the CNV group compared with the control group. Gray regions indicate areas of no significant difference after correction for multiple comparisons. Each vertex was adjusted for sex, site, age, and ICV. Ventral views are shown in Figure S6 in the online supplement. Covariance and overlap between surface and thickness at the vertex level are shown in Figure S7 in the online supplement. Panel C presents a comparison of effect sizes of CNVs on subcortical volume and shape metrics and previously published effect sizes on cognition and disease risk. Regression lines were fitted using the *geom_smooth* function in R. Pearson correlation and p values (using the parametric *cor.mtest* function in R) are shown for each metric. The x-axis reports the IQ loss (in IQ points) and the odds ratios for ASD or schizophrenia as reported in Table 1; the values range between 0 and 30. IQ loss (in IQ points) and odds ratio for ASD and schizophrenia risk were extracted from previous reports (3, 51). Plots excluding 22q11.2 loci, which showed similar results, are presented in Figure S8 in the online supplement. In addition, plots comparing the effect sizes of CNVs and the number of genes within CNV and the probability of being loss-of-function intolerant (pLI sum) for genes within CNV, as well as ICV metrics, are presented in Figure S9 in the online supplement. Concordance of effect sizes of CNVs on subcortical shape metrics and subcortical volume are shown in Figure SF10 in the online supplement. A=anterior; ASD=autism spectrum disorder; CAUD=caudate; CNV=copy number variant; DEL=deletion; DUP=duplication; FDR=false discovery rate; HIP=hippocampus; ICV=intracranial volume; L=left; P=posterior; PAL=pallidum; PUT=putamen; R=right; THAL=thalamus.

FIGURE 3. Correlations and principal component analysis across CNVs and NPDs[a]

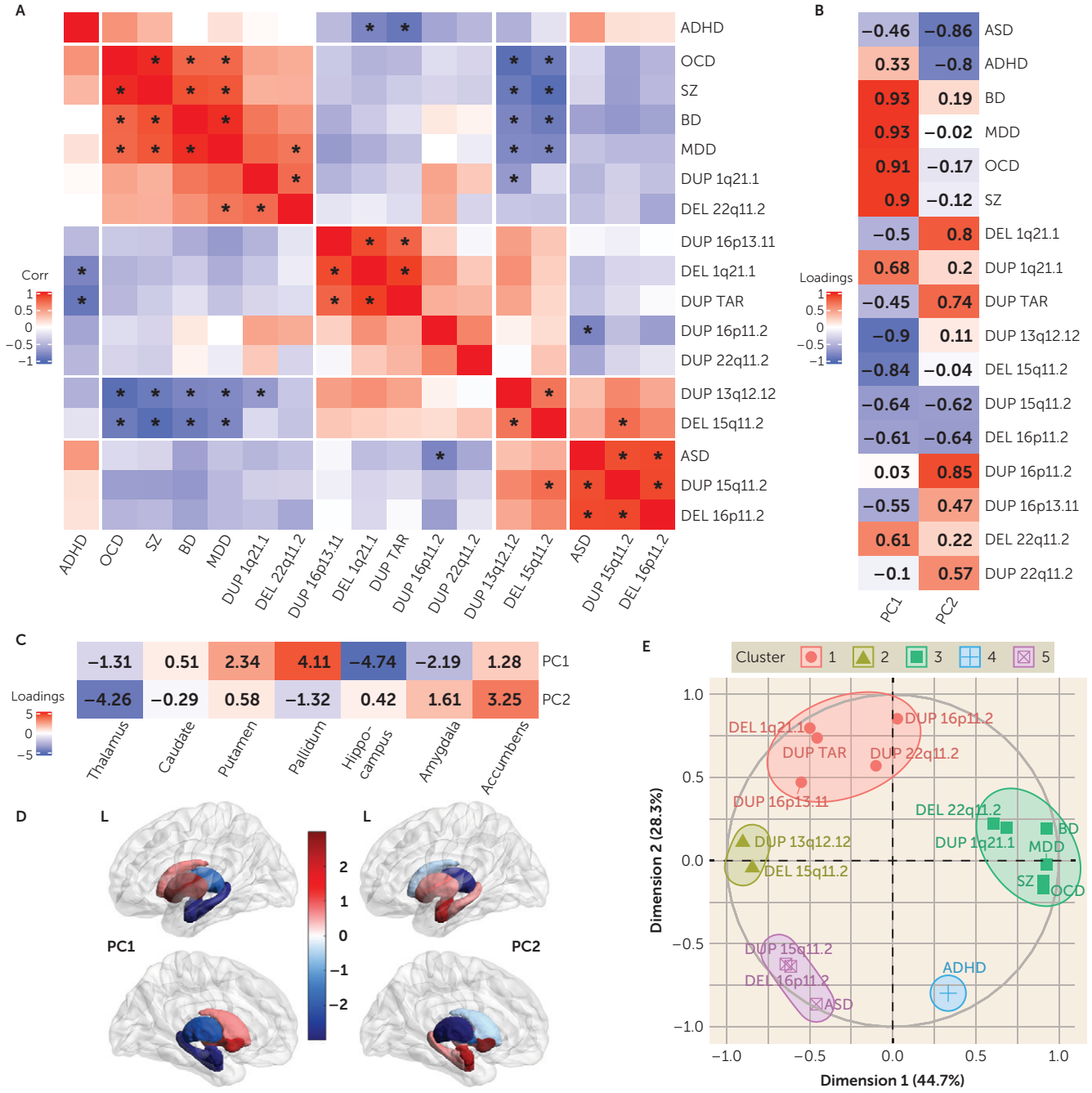

[a] Panel A shows correlations between Cohen's d profiles of CNVs and NPDs. Asterisks indicate p values <0.05 (using BrainSMASH). Five clusters identified by hierarchical (Ward distance) clustering are separated by white spaces. Panels B–E summarize principal component analysis across subcortical volumes of 11 CNVs and six NPDs. Panel B lists variable loadings on PC1 and PC2; panel C lists subcortical structures' loadings; panel D shows PC1 and PC2 loadings mapped on subcortical structures; and panel E is a correlation circle showing CNVs and NPDs in PC1 and PC2 space. CNV-NPD groupings were obtained using K-means clustering (k=5 clusters) in the PC space (Euclidean distance). ADHD=attention deficit hyperactivity disorder; ASD=autism spectrum disorder; BD=bipolar disorder; CNV=copy number variant; Corr=Pearson correlation; DEL=deletion; DUP=duplication; L=left hemisphere; MDD=major depressive disorder; NPD=neurodevelopmental and psychiatric disorder; OCD=obsessive-compulsive disorder; PC=principal component; SZ=schizophrenia.

and S16 in the online supplement). To formally test this hypothesis, we randomly sampled a smaller number of vertices and reran the principal component analysis. The resulting analysis shows that variance explained for surface+thickness by two principal components decreases from 52% (for 10 vertices), to 32% (1,000 vertices) and stabilizes from 1,000 to 2×27,200 vertices for surface+thickness (see Figure S17 in the online supplement).

FIGURE 4. Correlations and principal component analysis across vertex-wise Cohen's d maps of CNVs and NPDs[a]

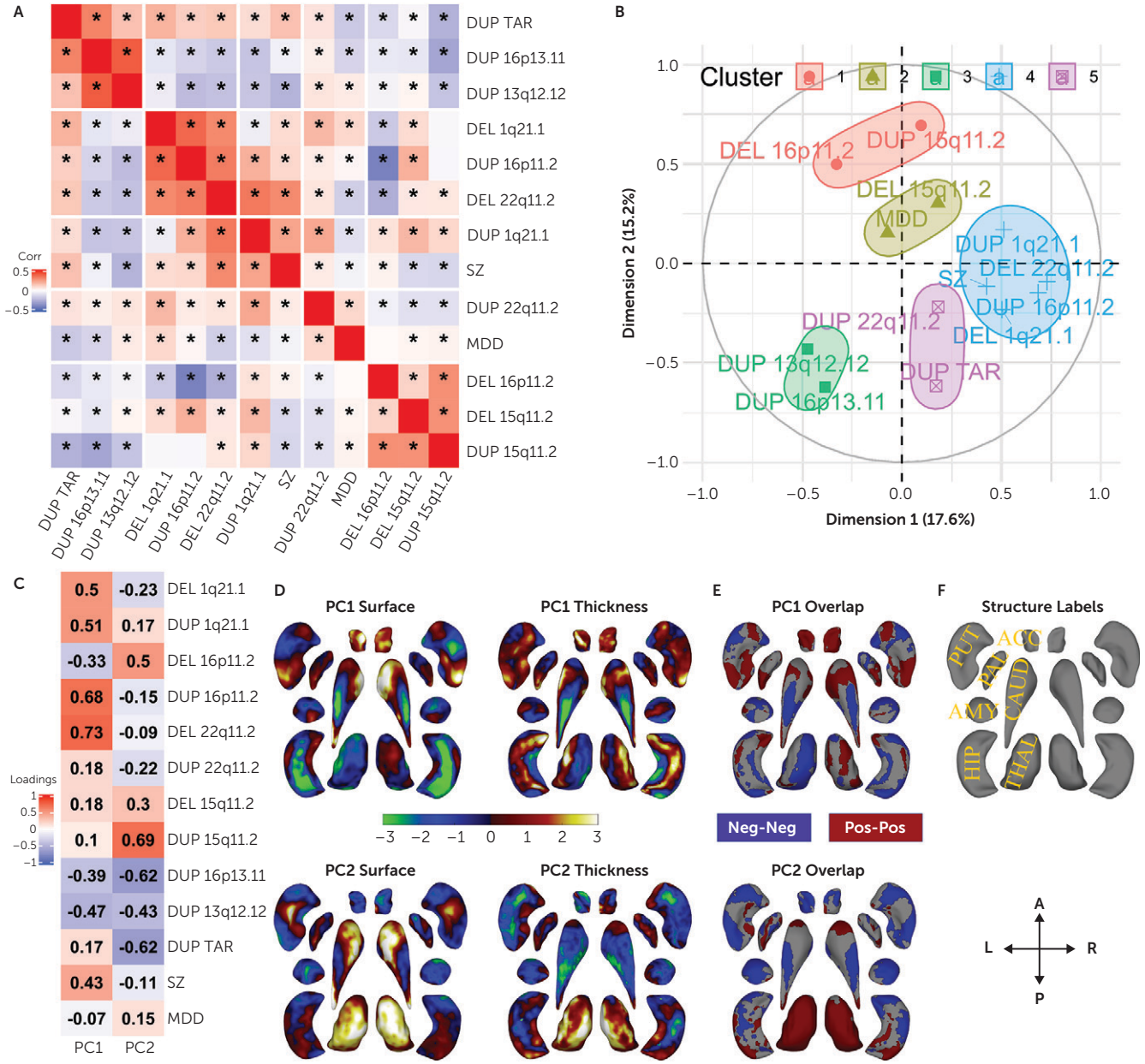

[a] Panel A shows correlations between vertex-wise Cohen's d profiles of CNVs and NPDs. Asterisks indicate p values <0.01 (parametric test). Five clusters identified by hierarchical (Ward distance) clustering are separated by white spaces. Panel B is a correlation circle with CNV and NPD clusters in PC1-PC2 space. Panel C lists CNV and NPD loadings of principal components 1 and 2. Panel D shows PC1 and PC2 brain maps (dorsal views); panel E shows the overlap of PCs of thickness and surface; and panel F provides the structures' labels and dorsal view directions. Thickness represents local radial distance, and surface represents local surface area dilation or contraction. Principal component analysis was run with CNVs as variables and vertices as observations (stacked across surface and thickness metrics and all subcortical structures; Z scored). For PC maps, blue/green and red/yellow colors indicate negative and positive coefficients, respectively. For overlap maps, blue and red represent negative-negative/positive-positive thickness and surface PC loadings at each vertex, respectively. Ventral views are shown in Figure S12 in the online supplement. A=anterior; ACC=accumbens; AMY=amygdala; CAUD=caudate; CNV=copy number variant; DEL=deletion; Dim=dimension; DUP=duplication; HIP=hippocampus; L=left; MDD=major depressive disorder; P=posterior; PAL=pallidum; PC=principal component; PUT=putamen; R=right; SZ=schizophrenia; THAL=thalamus.

DISCUSSION

In this large neuroimaging study characterizing and comparing subcortical alterations associated with 11 CNVs and six NPDs, we detected effects on subcortical volumes in nine of 11 CNVs. Analyses at a higher granularity using shape metrics showed that these effects were localized to subregions of the subcortical structures. The effect sizes of CNVs on subcortical structures were correlated with their previously reported effect sizes on cognition and risk for ASD and schizophrenia. That is, larger and gene-rich CNVs (e.g., 22q11.2 and 16p11.2-proximal), which show higher risk for

disease, also showed greater alterations of subcortical structures. Cohen's d values for CNVs were larger than those derived from case-control association studies for groups of individuals with a psychiatric condition. In line with the pleiotropic effects of CNVs on risk for multiple NPDs, we identified latent dimensions explaining 44.7% of the variance in Cohen's d maps across all CNVs and NPDs. Latent dimensions were defined by opposing loadings on basal ganglia and limbic structures.

Two CNVs—1q21.1 deletion and 15q11.2 duplication—showed FDR-significant effects on ICV only. The 15q11.2 duplication has not yet been associated with NPDs, so this is consistent with no detectable effects on subcortical volumes. The 1q21.1 deletion increases the risk for ASD and schizophrenia and decreases cognitive ability with moderate to mild effect sizes, and our study may therefore have been underpowered to detect its effects on subcortical structures.

All 11 CNVs showed significant effects on subcortical thickness and local surface area. The largest effects across metrics were observed for 22q11.2 deletions. Hippocampus volume was altered by five CNVs and had the largest number of significant vertices for surface across CNVs. The effect sizes of CNVs on volume, surface, and thickness were correlated with the previously reported mean effect size of each CNV on cognition and risk for disease. The same correlation has been reported between effect sizes of CNVs on functional connectivity metrics and cognition and risk for diseases (51). However, there was no relationship between effect sizes on ICV and risk for disease or cognition (14). When comparing across metrics, we found that the vertex-level shape analysis showed higher correlations, which suggests that increasing the granularity of analysis could enhance our understanding of the brain-behavior relationships. Studying brain-behavior relationships in unselected populations has proven to be challenging, and results have produced very small effect sizes (52). As opposed to fitting an average MRI pattern across a cognitive dimension, our alternative genetics-first approach provides a much stronger correlation by working with multiple MRI profiles associated with each genetic variant and its respective behavioral alterations. In other words, this allows one to move from single to multiple modes of brain-behavior associations.

Most of the variance in CNV-associated Cohen's d profiles for subcortical alterations was distinct for each CNV. This is consistent with a recent study showing relative specificity of CNV-associated morphometric cortical alterations (53). The amount of variance explained by the two top PCs (33%) across CNV-associated shape alterations is similar to that explained by latent dimensions (32% and 29%) previously published for cortical thickness and surface area across eight CNVs (54). These shared effects across CNVs, regardless of brain measures analyzed, suggest that CNVs may share some brain mechanisms. Overall, this may explain why CNVs may be associated with distinct clinical features while many also increase the risk for the same condition (36).

Extending the principal component analysis across CNVs and NPDs identified components similar to those described above, defined by opposing loadings on basal ganglia and limbic structures. Basal ganglia and limbic structures were previously identified as structures delineating different schizophrenia subtypes using data-driven approaches (34). These shared Cohen's d profiles may explain some of the pleiotropic effects of CNVs (i.e., why all NPD CNVs increase risk for either ASD or schizophrenia, or for both conditions). Subcortical structures with top PC loading include basal ganglia structures known to be primarily involved in motor control (55), as well as limbic structures involved in higher-order functions, including motivation, emotion, learning, and memory. This reflects an organization principle previously observed in the cortex from simple sensory processing to high-order processing regions (56, 57).

Our findings also suggest significant heterogeneity across CNVs and NPDs. CNVs showed either little or even negative correlations with NPDs. The latter tend to cluster among themselves, except for ASD and ADHD (37). For example, 16p11.2 duplications—which increase risk for schizophrenia and ASD—showed effects on subcortical shapes that were negatively correlated with those observed for idiopathic ASD. This could suggest that within a group of individuals with the same psychiatric diagnosis, some may show opposing MRI alterations. In addition, while effect sizes of CNVs on subcortical structures were correlated with risk, there was no concordance between the level of ASD or schizophrenia risk conferred by CNVs and the similarity between their subcortical profiles. This highlights, again, multiple modes of brain-behavior association underlying the heterogeneity of brain patterns associated with a psychiatric condition.

While some structures showed no significant differences at the gross volume level, shape analyses of the same structures revealed regions of lower as well as greater surface area and thickness. For example, while the volume of the caudate has small loading on PCs, subregions of the caudate were top contributors to PCs of shape metrics. This finding highlights the relevance of analyzing subcortical structures at the vertex level, which may identify alterations that are averaged out at the gross volumetric level.

Subregions of the hippocampus that were among the top contributors to the principal component analysis performed across CNVs were also previously reported in shape analysis of MDD (33) and schizophrenia (30). The observed shape differences have been reported to reflect patterns of neuronal deficits in postmortem studies of individuals with schizophrenia (30). For example, the mixed findings for caudate—increases and decreases for shape metrics in subregions—reflect findings from postmortem studies showing both larger (58) and smaller disease-related changes in total neuron number (59). The PC1 loadings of gross volume correlated with mean PC loadings for shape analysis, reflecting a consistent latent dimension. The microscopic reductions in neuron size or total number of neurons, which reflect shape differences, may manifest in macroscopic reductions in volume measured by MRI (30).

While shared variation could have been influenced by clinical ascertainment or psychiatric diagnoses, sensitivity

analyses showed that this is not the case, consistent with previous reports (54). Larger sample sizes with improved coverage across all age ranges would increase the accuracy of the normative modeling (60), as would better estimation of effect sizes for CNVs with small to moderate effect sizes. Direct comparison of shape metrics between CNVs and psychiatric conditions is required to identify latent dimensions across CNVs and conditions and will be the focus of future studies.

In summary, effect sizes of CNVs on subcortical structures were correlated with their effect size on cognition and risk for disease. Shape analyses highlighted subregional volume alterations that were averaged out in global volume analyses. Principal components captured common effects on subcortical volumes across CNVs, and NPDs may underlie some of the pleiotropic effects of CNVs. Basal ganglia and limbic structures that contributed to the latent dimension for volume are also those that contributed to the latent dimension for surface and thickness.

AUTHOR AND ARTICLE INFORMATION

Centre de Recherche du CHU Sainte-Justine, University of Montreal, Montreal (Kumar, Harvey, Huguet, Jean-Louis, Douard, Martin, Younis, Tamer, Dumas, Jacquemont); Mila–Quebec AI Institute, University of Montreal, Montreal (Dumas); Laboratoire de Recherche en Neuroimagerie, Department of Clinical Neurosciences (Modenato, Martin-Brevet, Lippé, Draganski), and Service des Troubles du Spectre de l'Autisme et Apparentés (Maillard, Rodriguez-Herreros, Pain), Centre Hospitalier Universitaire Vaudois and University of Lausanne, Lausanne, Switzerland; Human Genetics and Cognitive Functions, Institut Pasteur, and Université de Paris, CNRS UMR 3571, Paris (Moreau); Semel Institute for Neuroscience and Human Behavior, Departments of Psychiatry and Biobehavioral Sciences and Psychology, UCLA, Los Angeles (Kushan, Bearden); School for Mental Health and Neuroscience, Maastricht University, Maastricht, the Netherlands (Silva, Linden); Centre for Neuropsychiatric Genetics and Genomics (Silva, van den Bree, Owen, Hall), Division of Psychological Medicine and Clinical Neurosciences, School of Medicine (van den Bree, Owen, Hall), and Neuroscience and Mental Health Innovation Institute (van den Bree, Linden, Hall), Cardiff University, Cardiff, U.K.; Max Planck Institute for Human Cognitive and Brain Sciences, Leipzig, Germany (Draganski); Imaging Genetics Center, Mark and Mary Stevens Neuroimaging and Informatics Institute, Keck School of Medicine, University of Southern California, Marina del Rey (Ching, Moreau, Thompson); Department of Biomedical and Health Informatics, Children's Hospital of Philadelphia, Philadelphia (Schultz, Almasy); Lifespan Brain Institute, Children's Hospital of Philadelphia and Penn Medicine, Philadelphia (Schultz, Almasy); Department of Genetics, Perelman School of Medicine, University of Pennsylvania, Philadelphia (Almasy); Department of Psychiatry, Harvard Medical School, Boston, and Tommy Fuss Center for Neuropsychiatric Disease Research, Boston Children's Hospital, Boston (Glahn); Department of Biomedical Engineering, Duke University, Durham, N.C. (Isaev); Department of Biomedical Engineering, Oregon Health and Science University, Portland (Ragothaman); Department of Psychology, Georgia State University, Atlanta (Turner); Department of Psychiatry and Behavioral Sciences, Northwestern University Feinberg School of Medicine, Chicago (Alpert, Wang); Department of Psychiatry and Behavioral Health, Ohio State University Wexner Medical Center, Columbus (Wang); Department of Psychiatry and Behavioral Sciences and Department of Psychology, Stanford University, Stanford (Ho); Orygen, National Centre of Excellence in Youth Mental Health, Parkville, Australia, and Centre for Youth Mental Health, University of Melbourne, Melbourne (Schmaal); NORMENT, Division of Mental Health and Addiction, Oslo University Hospital, and University of Oslo, Oslo (Sønderby, Andreassen); Department of Medical Genetics, Oslo University Hospital, Oslo (Sønderby); K.G. Jebsen Centre for Neurodevelopmental Disorders, University of Oslo, Oslo (Sønderby, Andreassen); Department of Biomedical Engineering, Illinois Institute of Technology, Chicago (Gutman).

Send correspondence to Dr. Jacquemont (sebastien.jacquemont@umontreal.ca) and Dr. Kumar (kuldeep.kumar@umontreal.ca).

Dr. Kumar and Dr. Modenato contributed equally.

This research was supported by Calcul Québec (http://www.calculquebec.ca) and Compute Canada (http://www.computecanada.ca), the Brain Canada Multi-Investigator Research Initiative, NIMH (grant 1U01MH119690-01), the Canadian Institutes of Health Research (CIHR_400528), IVADO (Institut de Valorisation des Données) through the Canada First Research Excellence Fund, and Healthy Brains for Healthy Lives through the Canada First Research Excellence Fund. Dr. Jacquemont is a recipient of a Canada Research Chair in neurodevelopmental disorders and a chair from the Jeanne et Jean-Louis Levesque Foundation. The Cardiff CNV cohort was supported by the Wellcome Trust Strategic Award "DEFINE" and the National Centre for Mental Health with funds from Health and Care Research Wales (code 100202/Z/12/Z). The Centre Hospitalier Universitaire Vaudois (CHUV) cohort was supported by the Schweizerischer Nationalfonds (Swiss National Science Foundation) (Dr. Maillard, project PMPDP3 171331). Data from the UCLA cohort provided by Dr. Bearden (participants with 22q11.2 deletions or duplications and controls) were supported through grants from NIH (U54EB020403), NIMH (R01MH085953, R01MH100900, and R03MH105808), and the Simons Foundation Autism Research Initiative (SFARI Explorer Award). Dr. Modenato was supported by a Doc.Mobility grant from the Swiss National Science Foundation. Dr. Kumar was supported by the IVADO Postdoctoral Fellowship Program through the Canada First Research Excellence Fund. Dr. Ching and Dr. Thompson are supported in part by NIMH grants R01MH116147, R01MH123163, and R01MH121246, by the Milken Institute, and by the Baszucki Brain Research Fund. Dr. Sønderby is supported by the Research Council of Norway (grant 223273), the South-Eastern Norway Regional Health Authority (grant 2020060), the European Union's Horizon 2020 Research and Innovation Programme (CoMorMent project, grant 847776), and Kristian Gerhard Jebsen Stiftelsen (SKGJ-MED-021). Dr. Draganski is supported by the Swiss National Science Foundation (project grants 32003B_135679, 32003B_159780, 324730_192755, and CRSK-3_190185), ERA NET iSEE project, the Swiss Personalized Health Network SACR project, and the Leenaards Foundation. The Laboratoire de Recherche en Neuroimagerie receives support from the Roger De Spoelberch and Partridge Foundations.

The authors thank the families participating at the Simons Searchlight sites and the families who participated in the 16p11.2 European Consortium, as well as the Simons Searchlight Consortium, and express their appreciation for obtaining access to imaging and phenotypic data on SFARI Base.

Dr. van den Bree, Dr. Owen, and Dr. Hall have received grants from Takeda Pharmaceuticals. Dr. Owen has received a grant from Akrivia Health. Dr. Ching and Dr. Thompson have received a research grant from Biogen. Dr. Gutman is employed by and holds stock in Natera. The other authors report no financial relationships with commercial interests.

Data availability: UK Biobank data were downloaded under application 40980, and may be accessed via the standard data access procedure (http://www.ukbiobank.ac.uk/register-apply). UK Biobank CNVs were called using the pipeline developed in the Jacquemont Lab (https://github.com/labjacquemont/MIND-GENESPARALLELCNV); the final CNV calls are available for download from the UK Biobank returned data sets (Return ID: 3104, https://biobank.ndph.ox.ac.uk/ukb/dset.cgi?id=3104). Researchers may obtain the clinically ascertained data set described here by contacting Dr. Jacquemont (sebastien.jacquemont@umontreal.ca).

Approved researchers can obtain the Simons Searchlight population data set described here by applying at https://base.sfari.org.

Contributors to the Simons Searchlight Consortium (principal investigator, Wendy K. Chung) include the following: Hanalore Alupay, Benjamin Aaronson, Sean Ackerman, Katy Ankenman, Ayesha Anwar, Constance

Atwell, Alexandra Bowe, Arthur L. Beaudet, Marta Benedetti, Jessica Berg, Jeffrey Berman, Leandra N. Berry, Audrey L. Bibb, Lisa Blaskey, Jonathan Brennan, Christie M. Brewton, Randy Buckner, Polina Bukshpun, Jordan Burko, Phil Cali, Bettina Cerban, Yishin Chang, Maxwell Cheong, Vivian Chow, Zili Chu, Darina Chudnovskaya, Lauren Cornew, Corby Dale, John Dell, Allison G. Dempsey, Trent Deschamps, Rachel Earl, James Edgar, Jenna Elgin, Jennifer Endre Olson, Yolanda L. Evans, Anne Findlay, Gerald D. Fischbach, Charlie Fisk, Brieana Fregeau, Bill Gaetz, Leah Gaetz, Silvia Garza, Jennifer Gerdts, Orit Glenn, Sarah E. Gobuty, Rachel Golembski, Marion Greenup, Kory Heiken, Katherine Hines, Leighton Hinkley, Frank I. Jackson, Julian Jenkins III, Rita J. Jeremy, Kelly Johnson, Stephen M. Kanne, Sudha Kessler, Sarah Y. Khan, Matthew Ku, Emily Kuschner, Anna L. Laakman, Peter Lam, Morgan W. Lasala, Hana Lee, Kevin LaGuerre, Susan Levy, Alyss Lian Cavanagh, Ashlie V. Llorens, Katherine Loftus Campe, Tracy L. Luks, Elysa J. Marco, Stephen Martin, Alastair J. Martin, Gabriela Marzano, Christina Masson, Kathleen E. McGovern, Rebecca McNally Keehn, David T. Miller, Fiona K. Miller, Timothy J. Moss, Rebecca Murray, Srikantan S. Nagarajan, Kerri P. Nowell, Julia Owen, Andrea M. Paal, Alan Packer, Patricia Z. Page, Brianna M. Paul, Alana Peters, Danica Peterson, Annapurna Poduri, Nicholas J. Pojman, Ken Porche, Monica B. Proud, Saba Qasmieh, Melissa B. Ramocki, Beau Reilly, Timothy P.L. Roberts, Dennis Shaw, Tuhin Sinha, Bethanny Smith-Packard, Anne Snow Gallagher, Vivek Swarnakar, Tony Thieu, Christina Triantafallou, Roger Vaughan, Mari Wakahiro, Arianne Wallace, Tracey Ward, Julia Wenegrat, and Anne Wolken. Members of the European 16p11.2 Consortium (principal investigator, Sébastien Jacquemont) include the following: Marie-Claude Addor, Joris Andrieux, Benoît Arveiler, Geneviève Baujat, Frédérique Sloan-Béna, Marco Belfiore, Dominique Bonneau, Sonia Bouquillon, Odile Boute, Alfredo Brusco, Tiffany Busa, Jean-Hubert Caberg, Dominique Campion, Vanessa Colombert, Marie-Pierre Cordier, Albert David, François-Guillaume Debray, Marie-Ange Delrue, Martine Doco-Fenzy, Ulrike Dunkhase-Heinl, Patrick Edery, Christina Fagerberg, Laurence Faivre, Francesca Forzano, David Genevieve, Marion Gérard, Daniela Giachino, Agnès Guichet, Olivier Guillin, Delphine Héron, Bertrand Isidor, Aurélia Jacquette, Sylvie Jaillard, Hubert Journel, Boris Keren, Didier Lacombe, Sébastien Lebon, Cédric Le Caignec, Marie-Pierre Lemaître, James Lespinasse, Michèle Mathieu-Dramart, Sandra Mercier, Cyril Mignot, Chantal Missirian, Florence Petit, Kristina Pilekær Sørensen, Lucile Pinson, Ghislaine Plessis, Fabienne Prieur, Alexandre Raymond, Caroline Rooryck-Thambo, Massimiliano Rossi, Damien Sanlaville, Britta Schlott Kristiansen, Caroline Schluth-Bolard, Marianne Till, Mieke Van Haelst, and Lionel Van Maldergem.

Received April 5, 2022; revisions received October 24, 2022, and March 4, 2023; accepted April 28, 2023; published online July 12, 2023.

REFERENCES

1. Hibar DP, Stein JL, Renteria ME, et al: Common genetic variants influence human subcortical brain structures. Nature 2015; 520:224–229
2. Levitt JJ, Bobrow L, Lucia D, et al: A selective review of volumetric and morphometric imaging in schizophrenia. Curr Top Behav Neurosci 2010; 4:243–281
3. Jacquemont S, Huguet G, Klein M, et al: Genes to Mental Health (G2MH): a framework to map the combined effects of rare and common variants on dimensions of cognition and psychopathology. Am J Psychiatry 2022; 179:189–203
4. van Erp TGM, Hibar DP, Rasmussen JM, et al: Subcortical brain volume abnormalities in 2028 individuals with schizophrenia and 2540 healthy controls via the ENIGMA consortium. Mol Psychiatry 2016; 21:547–553
5. Schmaal L, Veltman DJ, van Erp TGM, et al: Subcortical brain alterations in major depressive disorder: findings from the ENIGMA Major Depressive Disorder working group. Mol Psychiatry 2016; 21: 806–812
6. Hibar DP, Westlye LT, van Erp TGM, et al: Subcortical volumetric abnormalities in bipolar disorder. Mol Psychiatry 2016; 21:1710–1716
7. Boedhoe PSW, Schmaal L, Abe Y, et al: Distinct subcortical volume alterations in pediatric and adult OCD: a worldwide meta- and mega-analysis. Am J Psychiatry 2017; 174:60–69
8. van Rooij D, Anagnostou E, Arango C, et al: Cortical and subcortical brain morphometry differences between patients with autism spectrum disorder and healthy individuals across the lifespan: results from the ENIGMA ASD working group. Am J Psychiatry 2018; 175:359–369
9. Hoogman M, Bralten J, Hibar DP, et al: Subcortical brain volume differences in participants with attention deficit hyperactivity disorder in children and adults: a cross-sectional mega-analysis. Lancet Psychiatry 2017; 4:310–319
10. Thompson PM, Jahanshad N, Ching CRK, et al: ENIGMA and global neuroscience: a decade of large-scale studies of the brain in health and disease across more than 40 countries. Transl Psychiatry 2020; 10:100
11. Cheon E, Bearden CE, Sun D, et al: Cross disorder comparisons of brain structure in schizophrenia, bipolar disorder, major depressive disorder, and 22q11.2 deletion syndrome: a review of ENIGMA findings. Psychiatry Clin Neurosci 2022; 76:140–161
12. Boedhoe PSW, van Rooij D, Hoogman M, et al: Subcortical brain volume, regional cortical thickness, and cortical surface area across disorders: findings from the ENIGMA ADHD, ASD, and OCD working groups. Am J Psychiatry 2020; 177: 834–843
13. Ching CRK, Gutman BA, Sun D, et al: Mapping subcortical brain alterations in 22q11.2 deletion syndrome: effects of deletion size and convergence with idiopathic neuropsychiatric illness. Am J Psychiatry 2020; 177:589–600
14. Modenato C, Martin-Brevet S, Moreau CA, et al: Lessons learned from neuroimaging studies of copy number variants: a systematic review. Biol Psychiatry 2021; 90:596–610
15. Marshall CR, Howrigan DP, Merico D, et al: Contribution of copy number variants to schizophrenia from a genome-wide study of 41,321 subjects. Nat Genet 2017; 49:27–35
16. Sanders SJ, Sahin M, Hostyk J, et al: A framework for the investigation of rare genetic disorders in neuropsychiatry. Nat Med 2019; 25:1477–1487
17. D'Angelo D, Lebon S, Chen Q, et al: Defining the effect of the 16p11.2 duplication on cognition, behavior, and medical comorbidities. JAMA Psychiatry 2016; 73:20–30
18. Chawner SJRA, Doherty JL, Anney RJL, et al: A genetics-first approach to dissecting the heterogeneity of autism: phenotypic comparison of autism risk copy number variants. Am J Psychiatry 2021; 178:77–86
19. Lin A, Vajdi A, Kushan-Wells L, et al: Reciprocal copy number variations at 22q11.2 produce distinct and convergent neurobehavioral impairments relevant for schizophrenia and autism spectrum disorder. Biol Psychiatry 2020; 88:260–272
20. Sanders SJ, He X, Willsey AJ, et al: Insights into autism spectrum disorder genomic architecture and biology from 71 risk loci. Neuron 2015; 87:1215–1233
21. Green EK, Rees E, Walters JTR, et al: Copy number variation in bipolar disorder. Mol Psychiatry 2016; 21:89–93
22. Charney AW, Stahl EA, Green EK, et al: Contribution of rare copy number variants to bipolar disorder risk is limited to schizoaffective cases. Biol Psychiatry 2019; 86:110–119
23. Kendall KM, Rees E, Bracher-Smith M, et al: Association of rare copy number variants with risk of depression. JAMA Psychiatry 2019; 76:818–825
24. Sønderby IE, van der Meer D, Moreau C, et al: 1q21.1 distal copy number variants are associated with cerebral and cognitive alterations in humans. Transl Psychiatry 2021; 11:182
25. Martin-Brevet S, Rodríguez-Herreros B, Nielsen JA, et al: Quantifying the effects of 16p11.2 copy number variants on brain structure: a multisite genetic-first study. Biol Psychiatry 2018; 84: 253–264

26. Sønderby IE, Gústafsson Ó, Doan NT, et al: Dose response of the 16p11.2 distal copy number variant on intracranial volume and basal ganglia. Mol Psychiatry 2020; 25:584–602
27. Writing Committee for the ENIGMA-CNV Working Group, van der Meer D, Sønderby IE, et al: Association of copy number variation of the 15q11. 2 BP1-BP2 region with cortical and subcortical morphology and cognition. JAMA Psychiatry 2020; 77:420–430
28. Sun D, Ching CRK, Lin A, et al: Large-scale mapping of cortical alterations in 22q11. 2 deletion syndrome: convergence with idiopathic psychosis and effects of deletion size. Mol Psychiatry 2020; 25:1822–1834
29. Fu Y, Zhang J, Li Y, et al: A novel pipeline leveraging surface-based features of small subcortical structures to classify individuals with autism spectrum disorder. Prog Neuropsychopharmacol Biol Psychiatry 2021; 104:109989
30. Gutman BA, van Erp TGM, Alpert K, et al: A meta-analysis of deep brain structural shape and asymmetry abnormalities in 2,833 individuals with schizophrenia compared with 3,929 healthy volunteers via the ENIGMA Consortium. Hum Brain Mapp 2022; 43: 352–372
31. Ge T, Reuter M, Winkler AM, et al: Multidimensional heritability analysis of neuroanatomical shape. Nat Commun 2016; 7:13291
32. Roshchupkin GV, Gutman BA, Vernooij MW, et al: Heritability of the shape of subcortical brain structures in the general population. Nat Commun 2016; 7:13738
33. Ho TC, Gutman B, Pozzi E, et al: Subcortical shape alterations in major depressive disorder: findings from the ENIGMA major depressive disorder working group. Hum Brain Mapp 2022; 43:341–351
34. Mamah D, Alpert KI, Barch DM, et al: Subcortical neuromorphometry in schizophrenia spectrum and bipolar disorders. Neuroimage Clin 2016; 11:276–286
35. Raznahan A, Won H, Glahn DC, et al: Convergence and divergence of rare genetic disorders on brain phenotypes: a review. JAMA Psychiatry 2022; 79:818–828
36. Moreno-De-Luca D, Martin CL: All for one and one for all: heterogeneity of genetic etiologies in neurodevelopmental psychiatric disorders. Curr Opin Genet Dev 2021; 68:71–78
37. Opel N, Goltermann J, Hermesdorf M, et al: Cross-disorder analysis of brain structural abnormalities in six major psychiatric disorders: a secondary analysis of mega- and meta-analytical findings from the ENIGMA Consortium. Biol Psychiatry 2020; 88:678–686
38. Huguet G, Schramm C, Douard E, et al: Genome-wide analysis of gene dosage in 24,092 individuals estimates that 10,000 genes modulate cognitive ability. Mol Psychiatry 2021; 26:2663–2676
39. Rees E, Walters JTR, Georgieva L, et al: Analysis of copy number variations at 15 schizophrenia-associated loci. Br J Psychiatry 2014; 204:108–114
40. Davies RW, Fiksinski AM, Breetvelt EJ, et al: Using common genetic variation to examine phenotypic expression and risk prediction in 22q11.2 deletion syndrome. Nat Med 2020; 26:1912–1918
41. Bernier R, Steinman KJ, Reilly B, et al: Clinical phenotype of the recurrent 1q21.1 copy-number variant. Genet Med 2016; 18:341–349
42. Jønch AE, Douard E, Moreau C, et al: Estimating the effect size of the 15Q11.2 BP1-BP2 deletion and its contribution to neurodevelopmental symptoms: recommendations for practice. J Med Genet 2019; 56: 701–710
43. Marquand AF, Kia SM, Zabihi M, et al: Conceptualizing mental disorders as deviations from normative functioning. Mol Psychiatry 2019; 24:1415–1424
44. Benjamini Y, Hochberg Y: Controlling the false discovery rate: a practical and powerful approach to multiple testing. J R Stat Soc 1995; 57:289–300
45. Burt JB, Helmer M, Shinn M, et al: Generative modeling of brain maps with spatial autocorrelation. Neuroimage 2020; 220:117038
46. Markello RD, Misic B: Comparing spatial null models for brain maps. Neuroimage 2021; 236:118052
47. Huguet G, Schramm C, Douard E, et al: Measuring and estimating the effect sizes of copy number variants on general intelligence in community-based samples. JAMA Psychiatry 2018; 75:447–457
48. Douard E, Zeribi A, Schramm C, et al: Effect sizes of deletions and duplications on autism risk across the genome. Am J Psychiatry 2021; 178:87–98
49. Chawner SJRA, Owen MJ, Holmans P, et al: Genotype-phenotype associations in children with copy number variants associated with high neuropsychiatric risk in the UK (IMAGINE-ID): a case-control cohort study. Lancet Psychiatry 2019; 6:493–505
50. Wainberg M, Merico D, Huguet G, et al: Deletion of loss-of-function–intolerant genes and risk of 5 psychiatric disorders. JAMA Psychiatry 2022; 79:78–81
51. Moreau CA, Harvey A, Kumar K, et al: Genetic heterogeneity shapes brain connectivity in psychiatry. Biol Psychiatry 2023; 93:45–58
52. Marek S, Tervo-Clemmens B, Calabro FJ, et al: Towards reproducible brain-wide association studies. bioRxiv, 2020. https://www.biorxiv.org/content/biorxiv/early/2020/08/22/2020.08.21.257758
53. Seidlitz J, Nadig A, Liu S, et al: Transcriptomic and cellular decoding of regional brain vulnerability to neurogenetic disorders. Nat Commun 2020; 11:3358
54. Modenato C, Kumar K, Moreau C, et al: Effects of eight neuropsychiatric copy number variants on human brain structure. Transl Psychiatry 2021; 11:399
55. Fahn S, Jankovic J, Hallett M: Functional neuroanatomy of the basal ganglia, in Principles and Practice of Movement Disorders, 2nd ed. New York, Elsevier, 2011, pp 55–65
56. Mesulam MM: From sensation to cognition. Brain 1998; 121: 1013–1052
57. Sydnor VJ, Larsen B, Bassett DS, et al: Neurodevelopment of the association cortices: patterns, mechanisms, and implications for psychopathology. Neuron 2021; 109:2820–2846
58. Beckmann H, Lauer M: The human striatum in schizophrenia, II: increased number of striatal neurons in schizophrenics. Psychiatry Res 1997; 68:99–109
59. Kreczmanski P, Heinsen H, Mantua V, et al: Volume, neuron density, and total neuron number in five subcortical regions in schizophrenia. Brain 2007; 130:678–692
60. Bethlehem RAI, Seidlitz J, White SR, et al: Brain charts for the human lifespan. Nature 2022; 604:525–533

Continuing Medical Education

You can earn CME credits by reading this article. Three articles in every *American Journal of Psychiatry* issue comprise a short course for up to 1 *AMA PRA Category 1 Credit*™ each. The course consists of reading the article and answering three multiple-choice questions with a single correct answer. CME credit is issued only online. Readers who want credit must subscribe to the AJP Continuing Medical Education Course Program (psychiatryonline.org/cme), select *The American Journal of Psychiatry* at that site, take the course(s) of their choosing, complete an evaluation form, and submit their answers for CME credit. A certificate for each course will be generated upon successful completion. This activity is sponsored by the American Psychiatric Association.

Examination Questions for "Subcortical Brain Alterations in Carriers of Genomic Copy Number Variants"

1. **What are the common subcortical volume alterations observed across most conditions and CNVs?**
   - A. A dimension characterized by opposing effects on the hippocampus/amygdala and putamen/pallidum, only across CNVs.
   - B. A dimension characterized by opposing effects on the hippocampus/amygdala and putamen/pallidum, across CNVs and across NPDs.
   - C. A dimension characterized by similar effects on the hippocampus/amygdala and putamen/pallidum, across CNVs and across NPDs.
   - D. A dimension characterized by similar effects on the hippocampus/amygdala and putamen/pallidum, only across CNVs.
2. **What is the correlation between effect sizes of CNVs on subcortical brain structures and their effect sizes on cognition and risk for ASD and schizophrenia?**
   - A. There is no correlation between effect sizes of CNVs on subcortical brain structures and their effect sizes on cognition and risk for ASD and schizophrenia.
   - B. Effect sizes of CNVs on subcortical brain structures are negatively correlated with their effect sizes on cognition and risk for ASD and schizophrenia.
   - C. Effect sizes of CNVs on subcortical brain structures are positively correlated with their effect sizes on cognition and risk for ASD and schizophrenia.
   - D. The study did not investigate the correlation between effect sizes of CNVs on subcortical brain structures and their effect sizes on cognition and risk for ASD and schizophrenia.
3. **Regarding the brain alterations associated with genetic risk for NPDs and idiopathic NPDs, which is the correct answer?**
   - A. The study's findings suggest that genetic risk for NPDs (CNVs) shows no similarities with idiopathic NPDs.
   - B. The study's findings suggest a relationship between the level of NPD risk conferred by CNVs and the similarity between their subcortical profiles
   - C. The study's findings suggest that all CNVs conferring risk for NPD tend to show subcortical alterations positively correlated with the subcortical alterations associated with the NPD.
   - D. The study's findings suggest the presence of heterogeneity in the relationships between CNVs and NPDs.